

Effective Baryon-Baryon Potentials in the Quark Delocalization and Color Screening Model

Jia-Lun Ping

Department of Physics, Nanjing Normal University, Nanjing, 210097, P. R. China

Fan Wang

Center for Theoretical Physics and Department of Physics, Nanjing University, Nanjing, 210008, P. R. China.

T. Goldman

*Theoretical Division, Los Alamos National Laboratory, Los Alamos, NM 87545, U.S.A
(September 14, 2018)*

Abstract

The quark delocalization and color screening model is used for a systematic study of the effective potential between baryons in the u, d and s sector. The model is constrained by the properties of baryons and N - N scattering. The effective potentials for the N - N ($IJ = 01, 10, 11, 00$) channels and the N - Λ and N - Σ ($IJ = \frac{1}{2}1, \frac{1}{2}0, \frac{3}{2}1, \frac{3}{2}0$) channels fit the N - N , N - Λ and N - Σ scattering data reasonably well. This model predicts: There are rather strong effective attractions between decuplet-baryons; the effective attractions between octet-baryons are weak or even repulsive; and the attractions between decuplet- and octet-baryons lie in between.

25.80.-e

25.10.+s

13.75.-n

25.40.-h

I. INTRODUCTION

Realistic models for baryon-baryon interactions are relevant to the study of the strong interaction, the understanding of properties of nuclei and hypernuclei, multiquark states, neutron stars, strangelets, strange matter and so on. A simple but realistic baryon-baryon potential is the basic input for any realistic calculation of hypernuclear properties and the equation of state of strongly interacting matter [1–3]. Such a potential is also needed for the study of dibaryons, as it is clear that an effective attraction between two baryons is necessary for the formation of a dibaryon, although it is not sufficient.

There are several approaches to obtaining the effective potential between baryons. One-boson-exchange-models, such as the Nijmegen and Jülich models [4], (although there are many others,) are a typical approach. The advantage of this approach is that it gives a very accurate description of the nucleon-nucleon (NN) interaction. For extension to the hyperon-nucleon (YN) interaction, the problem of too many unknown parameters (coupling constants) can be solved by imposing SU_3 flavor symmetry to constrain the coupling constants. The disadvantage is that a phenomenologically repulsive core, which is channel-dependent, has to be used.

Another approach [5–7] is based on applying the resonating group method (RGM) of calculation to quarks. Here, however, gluon exchange between the constituent quarks can only give the short range, repulsive core for the NN interaction. So in this model, meson exchange must be introduced to reproduce the medium and long range part of baryon-baryon interactions. It does have the advantage that the short range part is described by the quark model instead of a phenomenological repulsive core.

Although the experimental data can put some constraints on models of baryon-baryon interactions, the existing data, even including the newest data, still can not discriminate among most models. This is true because any disagreements with the newer data can generally be repaired by fine-tuning parameters, relaxing some of the constraints or making other adjustments in the models [8]. So in order to have a meaningful model for the baryon-baryon interaction with some predictive power, a model which is “parameter-free” is highly desirable.

Recently a new quark model, the quark delocalization, color screening model, (QDCSM) [9], has been developed. On comparison with the conventional quark cluster model, it is apparent that two new ingredients have been introduced. One is that the Hilbert space is enlarged to include fully confined and fully deconfined configurations as two extremes so that the actual configuration is determined variationally by the dynamics of the six quark system. The other is that the possible difference of the $q - q$ interaction inside a hadron (in an overall colorless state) and between quarks from two different colorless hadrons, due to the nonlinearity of QCD¹, is taken into consideration.

In this way, without introducing mesons, the long standing problem of the missing medium

¹For example, the contribution from gluons exchanged among three quarks which are in a color-singlet state is zero, while there is a nonzero contribution among three quarks which are in “colorful” state.

range attraction of NN forces in quark models is solved, and the parallel between nuclear and molecular forces obtains a natural explanation. The model has been successfully applied to describe NN scattering [9,10]. Using this model, a systematic search for dibaryon candidates within the three flavor world of u, d, s quarks was also made [11]. A relativistic model calculation obtains qualitatively similar results, even though the confinement mechanism differs. [12] Therefore, it seems worthwhile to apply this model to perform systematic and parameter free calculations of the effective baryon-baryon potentials. This paper is organized as follows: In section II, the model Hamiltonian and Hilbert space are described. Section III is devoted to a sketch of the calculation method. The results are given in section IV and a conclusion is given in section V.

II. QUARK DELOCALIZATION, COLOR SCREENING MODEL

The details of the model can be obtained from ref. [10,11]. Here we only give a brief review. For a single hadron, the QDCSM is same as the quark potential model, which has been successfully applied to describe the properties of baryons and mesons. The model Hamiltonian which describes a single baryon is written as

$$\begin{aligned} H(3) &= \sum_{i=1}^3 \left(m_i + \frac{p_i^2}{2m_i} \right) + \sum_{i < j=1}^3 V_{ij} - T_c(3), \\ V_{ij} &= V_{ij}^c + V_{ij}^G, \\ V_{ij}^c &= -\vec{\lambda}_i \cdot \vec{\lambda}_j a r_{ij}^n, \quad n = 1, 2, \\ V_{ij}^G &= \alpha_s \frac{\vec{\lambda}_i \cdot \vec{\lambda}_j}{4} \left[\frac{1}{r_{ij}} - \frac{\pi}{2} \left(\frac{1}{m_i^2} + \frac{1}{m_j^2} + \frac{4}{3m_i m_j} \vec{\sigma}_i \cdot \vec{\sigma}_j \right) \delta(\vec{r}_{ij}) + \dots \right]. \end{aligned} \quad (1)$$

The m_i , p_i and r_{ij} are quark masses, momenta and pairwise separations. The $\vec{\lambda}_i$ are color SU(3) Gell-Mann matrices and α_s is the strong coupling constant. For the confinement potential, V^c , both linear and quadratic forms are used in our calculations. In the effective one gluon exchange potential, V^G , only the color Coulomb and color magnetic terms are retained; other terms have been neglected temporarily [10] in order to reduce the calculational burden.

The wave function (WF) for a single baryon has the form

$$\psi(123) = \chi(123) \eta_{SIJ}(123) \phi(123). \quad (2)$$

Here $\chi(123)$ is the singlet color WF, $\eta_{SIJ}(123)$ is the symmetric spin-flavor $SU_{2 \times f}^{\sigma} \supset SU_f \times SU_2^{\sigma}$ WF (with S = strangeness, I = isospin, J = spin). The spatial wavefunction is given by

$$\begin{aligned} \phi(123) &= \phi_{1s}(\vec{r}_1) \phi_{1s}(\vec{r}_2) \phi_{1s}(\vec{r}_3), \\ \phi_{1s}(\vec{r}) &= \left(\frac{1}{\pi b^2} \right)^{\frac{3}{4}} e^{-\frac{(\vec{r}-\vec{s})^2}{2b^2}}, \end{aligned} \quad (3)$$

where \vec{s} is a reference center and b is a baryon size parameter.

For the two baryon system, we extend the Hamiltonian to

$$H(6) = \sum_{i=1}^6 (m_i + \frac{p_i^2}{2m_i}) + \sum_{i < j=1}^6 V_{ij} - T_c(6), \quad (4)$$

but modify the color confinement as follows:

$$V_{ij}^c = \begin{cases} -\vec{\lambda}_i \cdot \vec{\lambda}_j a r_{ij}^n & \text{if } i, j \text{ occur in the same baryon orbit,} \\ -\vec{\lambda}_i \cdot \vec{\lambda}_j \frac{a}{\mu_n} (1 - e^{-\mu_n r_{ij}^n}) & \text{if } i, j \text{ occur in different baryon orbit.} \end{cases} \quad (5)$$

Screened linear color confinement is found in lattice QCD calculations [13] and can be parametrized as

$$V(r) = \left(-\frac{\alpha_s}{r} + \sigma r \right) \left(\frac{1 - e^{-\mu_1 r}}{\mu_1 r} \right), \quad (6)$$

with $\alpha_s = 0.21 \pm 0.01$, $\sqrt{\sigma} = 400 \text{ MeV}$, $\mu_1^{-1} = 0.90 \pm 0.20 \text{ fm}$.

For the two baryon wave function, we extend the quark cluster model space by introducing delocalized single quark orbits:

$$\begin{aligned} \psi_L(\vec{r}) &= (\phi_L(\vec{r}) + \epsilon(s)\phi_R(\vec{r})) / N(s), \\ \psi_R(\vec{r}) &= (\phi_R(\vec{r}) + \epsilon(s)\phi_L(\vec{r})) / N(s), \\ N^2(s) &= 1 + \epsilon^2(s) + 2\epsilon(s)\langle\phi_L|\phi_R\rangle. \end{aligned} \quad (7)$$

where ϕ_L, ϕ_R are the quark cluster bases of the type described above for individual baryons:

$$\begin{aligned} \phi_L(\vec{r}) &= \left(\frac{1}{\pi b^2} \right)^{\frac{3}{4}} e^{-\frac{(\vec{r}+\vec{s}/2)^2}{2b^2}} && \text{(left centered orbit),} \\ \phi_R(\vec{r}) &= \left(\frac{1}{\pi b^2} \right)^{\frac{3}{4}} e^{-\frac{(\vec{r}-\vec{s}/2)^2}{2b^2}} && \text{(right centered orbit).} \end{aligned} \quad (8)$$

Here \vec{s} is the separation between the centers of two q^3 clusters. The delocalization parameter $\epsilon(s)$ is determined variationally for every $s = |\vec{s}|$ by the q^6 dynamics (see section III). The quark molecular orbit introduced by Fl. Stancu and L. Wilets [14] is a restricted version of this structure.

The two baryon wave function is written as

$$\begin{aligned} \Psi_{\alpha_1 F_1, \alpha_2 F_2}^\alpha(1 \cdots 6) &= \mathcal{A}[\psi_{\alpha_1 F_1}(123)\psi_{\alpha_2 F_2}(456)]_\alpha, \\ \psi_{\alpha_1 F_1}(123) &= \chi(123)\eta_{S_1 I_1 J_1 F_1}(123)\psi_L(1)\psi_L(2)\psi_L(3) \\ \psi_{\alpha_2 F_2}(456) &= \chi(456)\eta_{S_2 I_2 J_2 F_2}(456)\psi_R(4)\psi_R(5)\psi_R(6). \end{aligned} \quad (9)$$

Here $\alpha = (S I J)$ are again the strong interaction conserved quantum numbers: strangeness, isospin and spin. (Orbital angular momentum is assumed to be zero for the lowest states. In principle, an angular momentum projection should be done but we leave this for future refinement.) The q^3 cluster WF is almost the same as given in Eq.(2), but the single cluster Gaussian WF, Eq.(3), is replaced by the delocalized orbital WF, eq.(7). Finally, \mathcal{A} is the normalized antisymmetry operator

$$\mathcal{A} = \frac{1}{\sqrt{20}} \sum (-)^{\delta_p} p$$

The model parameters m, m_s, b, α_s, a are fixed by the spectrum of baryons; μ_1 is taken from lattice gauge QCD calculations; and μ_2 is fixed by fitting the N - N phase shifts. The fitted parameters are given in Table I.

Table I. The parameters used in the calculations.

	m (MeV)	m_s (MeV)	b (fm)	α_s	a (MeV·fm $^{-2}$)	μ_n
$n = 1$	313	618.45	0.625	1.71	39.14	1.1
$n = 2$	313	633.76	0.603	1.54	25.13	1.6

III. CALCULATION METHOD

Since the relative motion between two baryons is rather slow compared to the internal motion of the quarks in the baryons and the quantum fluctuation of the center of mass coordinates of the baryons is neglected temporarily (again leaving refinement for the future), we can define the effective baryon-baryon potential as follows:

$$V_\alpha(s_0) = E_6(s = s_0) - E_6(s = \infty) \quad (10)$$

where $E_6(s)$ is the energy of two baryon system at separation s , which can be obtained by calculating the matrix elements of the Hamiltonian, Eq.(4), in the baryon states, Eq.(9). In the nonrelativistic approximation,

$$E_6(s) = E_3(123) + E_3(456) + E_{rel} + V_\alpha(s), \quad (11)$$

where E_3 is the total energy of a single baryon and E_{rel} is the energy of relative motion of two baryons. When $s \rightarrow \infty$, we must have $V_\alpha \rightarrow 0$, so

$$E_6(s = \infty) = E_3(123) + E_3(456) + E_{rel}. \quad (12)$$

Note that the six-quark WF decomposition maintains a non-zero E_{rel} even at ∞ and it is our assumption that this constant is the appropriate quantity to remove at finite s which leads to the expression for $V_\alpha(s)$ shown in Eq.(10).

The treatment of the center of mass motion merits some additional discussion. In order to have a correct separation of total kinetic energy into internal, relative and center of mass parts in the asymptotic region, we redefined the CM energy using an average of the single quark mass

$$T_c(n) = \frac{1}{2M_n} \left(\sum_{i=1}^n \vec{p}_i \right)^2 = \frac{1}{2} \left(\frac{n - n_s}{n} \frac{1}{m} + \frac{n_s}{n} \frac{1}{m_s} \right) \left(\sum_{i=1}^n \vec{p}_i \right)^2, \quad (13)$$

where n and n_s are total number of quarks and s -quarks in the system, respectively. In this way, the kinetic energy is free from CM motion when an SU(3)-flavor symmetric wave function is used.

$$T(n) = \sum_{i=1}^n \frac{1}{2m_i} \vec{p}_i^2 - T_c(n) = \frac{1}{2nm} \left(\frac{n - n_s}{n} + \frac{n_s}{n} \frac{m}{m_s} \right) \sum_{i>j=1}^n (\vec{p}_i - \vec{p}_j)^2 \quad (14)$$

A similar treatment can be found in ref. [7].

To calculate the matrix elements of H in the basis given by Eq.(9) is a daunting task, especially for a systematic search, where many matrix elements must be evaluated. So a group theory method was developed to relate the physical basis to a group chain classification basis (symmetry basis). In the symmetry basis, the well known fractional parentage expansion can be used. The calculation of six-body matrix elements reduces to two-body matrix elements and four-body overlaps. For details of the method, see ref. [15]. In order to discern the effect of channel coupling, a channel potential is introduced. For a given set of quantum numbers $\alpha = (S I J)$, the effective channel potentials are defined by the same formula Eq.(10), where $E_6(s = s_0)$ and $E_6(s = \infty)$ are the eigenenergies of the two baryon system at separation s_0 and ∞ , respectively, which can be obtained by diagonalizing the q^6 Hamiltonian. The eigenstates are expressed as multiple physical channel coupling wave functions

$$\Psi_\alpha(1 \cdots 6) = \sum_{\alpha_1 F_1, \alpha_2 F_2} C_{\alpha_1 F_1, \alpha_2 F_2}^\alpha \Psi_{\alpha_1 F_1, \alpha_2 F_2}^\alpha. \quad (15)$$

The channel coupling coefficients $C_{\alpha_1 F_1, \alpha_2 F_2}^\alpha$ are determined by the diagonalization. In general, we can identify which of the baryon channels an eigenenergy corresponds to by finding which baryon channel for that eigenenergy has the largest channel coupling coefficient. Although this identification is not unique, it guarantees that the channel energy varies smoothly with s_0 . Where no coefficient is discernably dominant, we examine the energies at (nearby) larger and smaller values of s_0 and again choose the value which provides for a smooth continuation of the channel energy. This replaces an earlier procedure we used which involved choosing the lowest eigenenergy available. This older procedure had the disadvantage of not having a clear relation to particular baryon-baryon channels, of introducing sharp (discontinuous in the derivative with respect to s_0) changes in the energy, and of prohibiting the identification of any but the lowest energy channel. The energies obtained in this way depend on the separation s and the delocalization parameter $\epsilon(s)$. We repeat the calculation for each s by varying $\epsilon(s)$ from 0.01-1.0 with 0.01 stepsize to obtain the minimum of the lowest eigenenergy. At the same time, the delocalization parameter $\epsilon(s)$ and all eigenenergies are determined.

IV. RESULTS

The effective potential between combinations of octet- and decuplet-baryons (168 channels, altogether) were calculated. To save space, only a few typical examples are shown in Figs.1-7. (We will be happy to provide any of the others upon request.)

Fig.1a shows the effective N - N potential for channels $(I J) = (01), (10), (11)$ and (00) with the quadratic color confinement interaction. Clearly there is an effective attraction in the first two channels, with (01) a little stronger than (10) . The other two channels are repulsive. These potentials are quite similar to phenomenological N - N potentials such as the Reid soft core N - N potential. [16] However, when we proceed to a dynamical calculation of the phase shifts, we must also perform a partial wave decomposition and make a center of mass correction of the kernel of the interaction Hamiltonian. The net

effect of these calculations is to create some additional attraction, so that a slight reduction of the value of the screening parameter is then needed to produce good agreement with the results of N - N phase shift analyses. [17]

Fig.1b is similar to Fig.1a but with the linear color confinement interaction. Comparison of Fig.1a with Fig.1b makes it clear that both sets of potentials have qualitatively the same pattern, but with a weaker attraction for the case of linear confinement. In fact, we find that for the linear color confinement interaction, the potentials in these four channels agree reasonably well [18] with the phase shift analyses *without any change from the lattice QCD value of the screening parameter* [13]. In this sense, our results provide a parameter-free prediction of the phase shifts in these channels.

The channel coupling calculation shows that channel coupling produces minor effects for the N - N channels, and so we do not present those results here. In the following, we only present the results with quadratic color confinement to save space.

Figs.2-3 shows the results for N - Σ and N - Λ channels. For N - Λ , the spin triplet state is a little more attractive than the spin singlet; the channel coupling adds a bit more attraction to this state but leaves the spin singlet almost unchanged. We note that $^4_\Lambda H$ and $^4_\Lambda He$ both have spin zero ground states and spin one excited states. One might interpret this as evidence that the spin-singlet N - Λ interaction is more attractive than the spin triplet. However, the situation is not so transparent due to the complications of the interactions of the four bodies involved and, in addition, Λ - Σ^0 mixing effects. The spin one ground state of the deuteron is certainly an indication that the spin triplet N - N interaction is more attractive than the spin triplet, and we might reasonably expect (by flavor symmetry) that this should hold true for all octet-baryon combinations. However, due to the strong tensor interaction from pion exchange, the Nijmegen OBE model F [4] nonetheless includes a more attractive spin singlet N - N central interaction. Furthermore, there is a paucity of direct data on scattering in the Y - N channels, and widely differing relative strengths for the central interaction are all consistent with both the available data and the nuclear states referred to above. The QDCSM, on the other hand, predicts that spin triplet N - N and N - Λ interactions are stronger than spin singlet ones. Clearly, which central interaction is stronger in each case merits additional study.

For N - Σ , we find the strongest attraction in the $IJ = \frac{1}{2}1$ channel, while the $IJ = \frac{3}{2}0$, and $\frac{1}{2}0$ channels both have a little weaker attraction (single channel case), and the $IJ = \frac{3}{2}1$ channel is repulsive. Channel coupling has little effect on $\frac{1}{2}1$, and pushes $\frac{1}{2}0$ from attractive to repulsive. These show that the N - Σ potential is more strongly spin and/or isospin dependent than the N - Λ potentials, which have a little weaker dependence on spin. These results are in qualitative agreement with the calculations of OBE models [4] and hybrid quark model calculations [6], except that our attraction for the N - $\Sigma(\frac{1}{2}1)$ channel is too strong. It is worth noting that the N - $\Sigma(\frac{3}{2}1)$ channel has a small bump at $R_s \sim 1.3$ fm. The reason for this is not clear, but it seems to correspond to the statement of ref. [6], that the repulsion between two clusters has its maximum not at distance zero, but at a finite cluster distance.

For all other channels, some general features of the effective potential have been found in this calculation: An effective attraction exists in most channels. The attraction is very strong between two decuplet-baryons, but the attraction is very weak and even repulsive between octet-baryons, while the strength of the attraction between octet- and

decuplet-baryons lies in between. The reason is that in a decuplet baryon, spin is totally symmetric and color is totally antisymmetric, so that the hyperfine interaction is purely repulsive. For a six quark system, the spin and color are neither totally symmetric nor antisymmetric, leading to the hyperfine interaction not always being repulsive, and so providing an effective attraction.

Some states are forbidden for structureless baryons by the Pauli principle: $\Delta\Delta(IJ = 33)$, $\Delta\Sigma^*(\frac{5}{2}3)$, $\Sigma^*\Xi^*(\frac{1}{2}3)$, $\Omega\Omega(03)$. For these states, we find that the energy of the system becomes very large when the distance between the two baryons tends to zero (see Fig.4). Because the effective B - B interactions are directly related to multiquark states, in the following we present the baryon-baryon potential along with a discussion regarding dibaryon states.

(a) States with only non-strange quarks. Since the states in this part do not contain any strange quarks, they are not affected by symmetry breaking.

Clearly many channels have an effective attraction, but to form bound states one has to consider not only two body decay modes, but also many body decay modes. For example, for a $\Delta\Delta$ channel to form a narrow dibaryon resonance, the energy of dibaryon should not only be less than the sum of the masses of two Δ s, but it should also be less than the sum of the masses of two nucleons and two pions because each Δ itself can decay into $N\pi$. In addition, the zero-point harmonic oscillator energy must be added to the system. Only channels with sufficient attraction can form bound states or narrow resonances.

The interesting states are:

$NN(01)$, $NN(10)$ and $\Delta\Delta(03)$. The $NN(01)$ state is a loosely bound state: This is just the deuteron, which is reproduced here. The $NN(10)$ state corresponds to the known NN zero energy resonance. The $\Delta\Delta(03)$, called d^* , is a narrow resonance. [19] Although the $\Delta\Delta(01)$ channel is more attractive than the $\Delta\Delta(03)$ (see Fig.5), it couples strongly to $NN(01)$, so it is not a good candidate for an observable dibaryon. Conversely, because the $\Delta\Delta(03)$ has a large angular momentum, it cannot couple to an NN s -wave state, or to $N\Delta$ (also forbidden by isospin) directly. The large angular momentum hinders the decay to NN , and the energy of the state prevents its decay to $NN\pi\pi$, so it is a good candidate for a narrow resonance. [20]

(b) States with one or more strange quarks. The general features stay the same for states with strange quarks. There are also several particularly interesting states (see Figs.6-8). $\Sigma\Sigma(20)$, $\Xi\Xi(00)$ are both deuteron-like states, consisting of two octet-baryons, which have a weak attraction and the minima of their potentials are found at rather large separations (> 1 fm). Channel coupling has a minor effect on the results. These are possible dibaryon candidates but are sensitive to model details.

It is worth mentioning the $\Omega\Omega(00)$ state. In our calculations, its effective attraction is not weak, but rather strong enough to form a strong interaction bound state. Because it consists of two Ω s and Ω is strong interaction stable, it is a good candidate for a dibaryon, although it is also sensitive to model details. In addition, it may be too difficult to produce this state even in relativistic heavy ion collision experiments.

The H particle ($YIJ = 000$) is a special state in our calculation. The channel coupling calculation (see Fig.6) shows that it is a six quark state consisting mainly of octet-baryons (dominant components are $N\Xi$ and $\Sigma\Sigma$) that has an attraction that is not too weak. It is possible that it appears as a dibaryon.

The states $YIJ = -1\frac{1}{2}2$ and $-1\frac{1}{2}1$ both have a rather strong attraction. However, when channel coupling is taken into account, the attraction is greatly reduced for the $J = 1$ channel, whereas the $J = 2$ channel is almost unaffected. Although they consist of octet- and decuplet-baryons, their energies are lower than the $\Lambda\Xi\pi$ three body decay channels. A dibaryon may form in the state $YIJ = -1\frac{1}{2}2$.

V. CONCLUSION

Taking into account both color screening and quark delocalization, a systematic study of the effective baryon-baryon potentials has been performed by using a quark cluster model. The model parameters were fixed by baryon properties and the color screening parameter was taken from lattice gauge QCD calculations for linear confinement (or from N - N scattering data for quadratic confinement). Consequently, the calculated baryon-baryon potentials can be viewed as a parameter free result. As a general trend, we find that a very strong attraction exists between two decuplet-baryons. For decuplet and octet baryons, one has a mild attraction. Very weak attraction, or even repulsion appears in the octet-octet baryon system.

Because the "predicted" N - N , N - Λ and N - Σ effective potentials fit the scattering data reasonably well, we expect that the other baryon-baryon effective potentials are reasonable predictions as well. At least for those cases for which one has neither any experimental data nor good theoretical models, our model results should be useful intermediate guides for studies of such exotics as multiquark states, strangelets and of the equation of state of strongly interacting matter in relativistic heavy ion collisions, where multistrange baryons constitute a significant component.

For a dibaryon search, these results suggest that experiments should focus on octet-octet systems with low spin and decuplet-decuplet systems with high spin. For octet-octet systems, there are dibaryon candidates which are loosely bound but stable against strong interaction decay and have small quark delocalization. This is the nuclear type of dibaryon and the deuteron is a typical example. For decuplet-decuplet systems, the most striking resonances are states with high spin and large quark delocalization. These are a quark matter type of dibaryon and the d^* is a typical example.

Strangeness conserving transition potentials (e.g., $N\Lambda \rightarrow N\Sigma$) can also be obtained in our model. We defer discussion of those results to a later paper.

We thank R. Timmermans for a useful conversation. This research is supported in part by the Department of Energy under contract W-7405-ENG-36 and in part by the National Science Foundation of China.

REFERENCES

- [1] B. F. Gibson and E. V. Hungerford, Phys. Rep. **257**, 349 (1995) and references therein.
- [2] C. B. Dover, D. J. Millener and A. Gal, Phys. Rep. **184**, 1 (1989).
- [3] G. E. Brown, Phys. Rep. **163**, 167 (1988); S. Balberg and A. Gal, nucl-th/9704013 and references therein.
- [4] R. Machleidt, K. Holinde and Ch. Elster, Phys. Rep. **149**, 1 (1987); M. M. Nagels, T. A. Rijken and J. J. de Swart, Ann. Phys. **79**, 338 (1973); Phys. Rev. **D 12**, 744 (1975); **D15**, 2547 (1977); W. N. Cottingham *et al*, Phys. Rev. **D8**, 800 (1973); P. M. M. Maessen, T. A. Rijken and J. J. de Swart, Phys. Rev. **C40**, 2226 (1989); B. Holzenkamp, K. Holinde and J. Speth, Nucl. Phys. **A500**, 485 (1989).
- [5] M. Oka, K. Shimizu and K. Yazaki, Nucl. Phys. **A464**, 700 (1987); Y. Koike, K. Shimizu and K. Yazaki, Nucl. Phys. **A513**, 653 (1990); K. Shimizu, Rep. Prog. Phys. **52**, 1 (1989); K. Yazaki, in *Properties and interactions of hyperons*, ed. B. F. Gibson *et al*, (World Scientific, Singapore, 1994), p.189.
- [6] U. Straub, Z. Y. Zhang, K. Bräuer, A. Faessler, S. H. Khadkikar and G. Lübeck, Nucl. Phys. **A 483**, 686 (1988); U. Straub *et al*, Phys. Lett. **B200**, 241 (1988).
- [7] Y. Fujiwara, C. Nakamoto and Y. Suzuki, Phys. Rev. Lett. **76**, 2242 (1996); Prog. Theor. Phys. **94**, 215 (1995); **94**, 353 (1995); C. Nakamoto, Y. Suzuki and Y. Fujiwara, Prog. Theor. Phys. **94**, 65 (1995).
- [8] R. Timmermans, in *Properties and Interactions of hyperons*, ed. B. F. Gibson *et al*, (World Scientific, Singapore, 1994), p.179.
- [9] F. Wang, G. H. Wu, L. J. Teng and T. Goldman, Phys. Rev. Lett. **69**, 2901 (1992).
- [10] G. H. Wu, L. J. Teng, J. L. Ping, F. Wang and T. Goldman, Phys. Rev. **C53**, 1161 (1996).
- [11] F. Wang, J. L. Ping, G. H. Wu, L. J. Teng and T. Goldman, Phys. Rev. **C51**, 3411 (1995).
- [12] T. Goldman, K. Maltman, G. J. Stephenson, Jr., J. L. Ping and F. Wang, Mod. Phys. Lett. **A13**, 59 (1998).
- [13] K. D. Born, *et al*, Phys. Rev. **D 40**, 1653 (1989).
- [14] Fl. Stancu and L. Wilets, Phys. Rev. **C 36**, 726 (1987).
- [15] F. Wang, J. L. Ping and T. Goldman, Phys. Rev. **C51**, 1648 (1995).
- [16] R. V. Reid, Jr., Ann. Phys. **50**, 411 (1968).
- [17] G. H. Wu, L. J. Teng, J. L. Ping, F. Wang and T. Goldman, Mod. Phys. Lett. **A10**, 1895 (1995).
- [18] G. H. Wu, J. L. Ping, L. J. Teng, F. Wang and T. Goldman, "Quark Delocalization Color Screening Model and Nucleon-Baryon Scattering", (in preparation).
- [19] T. Goldman, K. Maltman, G. J. Stephenson, Jr., K. E. Schmidt and F. Wang, Phys. Rev. **C39**, 1889 (1989).
- [20] C. W. Wong, Phys. Rev. **C57**, 1962 (1998).

FIGURE CAPTIONS

Fig. 1a Effective potential in MeV vs. baryon separation in fm for N-N channels with quadratic confinement.

Fig. 1b Same as in Fig. 1a, but with linear confinement.

Fig. 2 Effective potential in MeV vs. baryon separation in fm for $N-\Sigma$ channels with and without channel coupling.

Fig. 3 Effective potential in MeV vs. baryon separation in fm for $N-\Lambda$ channels with and without channel coupling.

Fig. 4 Effective potential in MeV vs. baryon separation in fm for various forbidden states.

Fig. 5 Effective potential in MeV vs. baryon separation in fm for $\Delta-\Delta$ channels.

Fig. 6 Effective potential in MeV vs. baryon separation in fm for $YIJ = 000$ channels (i.e., with two strange quarks) with and without channel coupling.

Fig. 7 Effective potential in MeV vs. baryon separation in fm for $N-\Omega$ channels with and without channel coupling.

Fig. 8 Effective potential in MeV vs. baryon separation in fm for $\Sigma\Sigma, \Xi\Xi$ and $\Omega\Omega$ channels.

Fig.1a. Effective potential
(for NN with quadratic confinement)

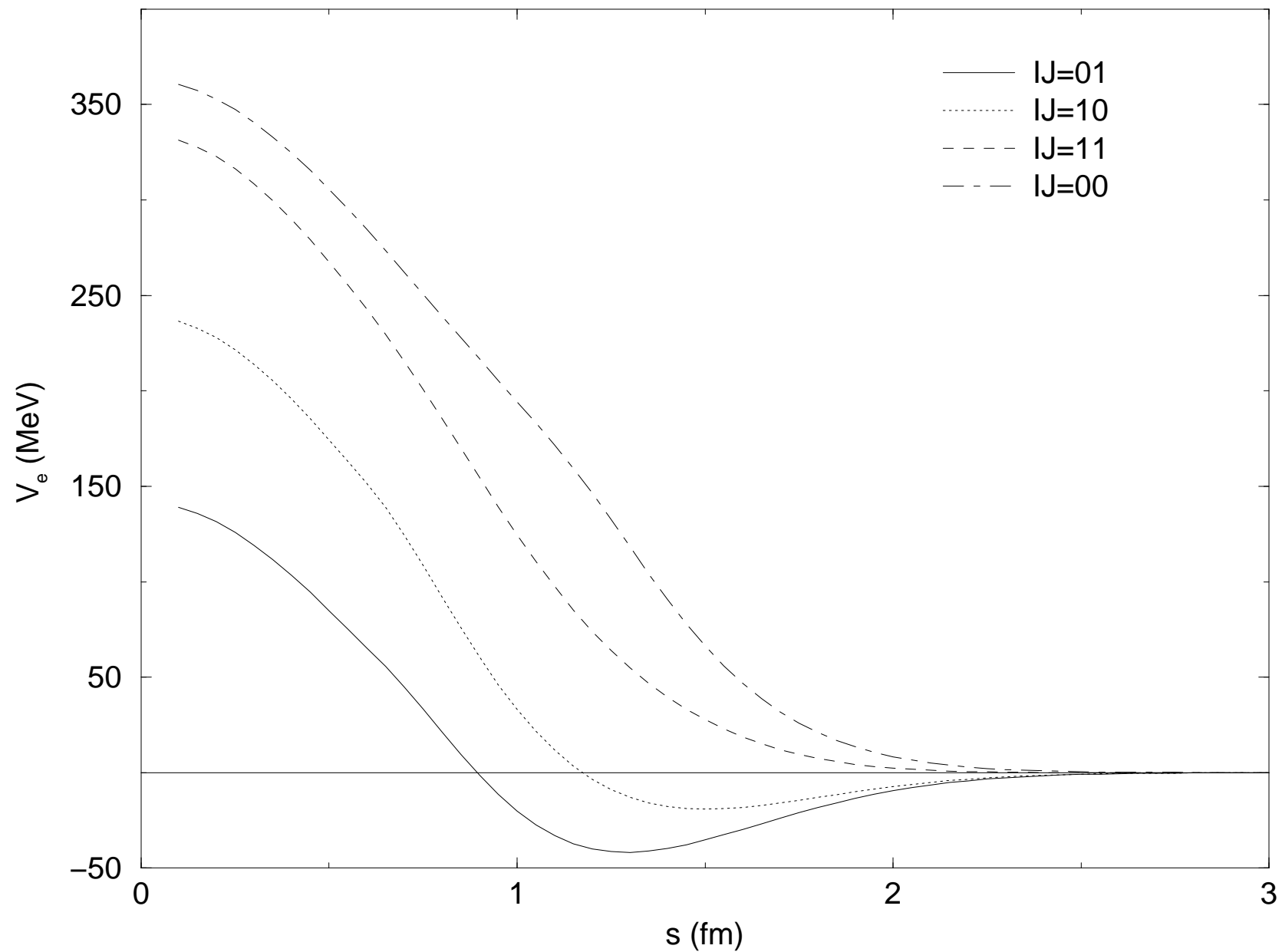


Fig.1b. Effective potential
(for NN with linear confinement)

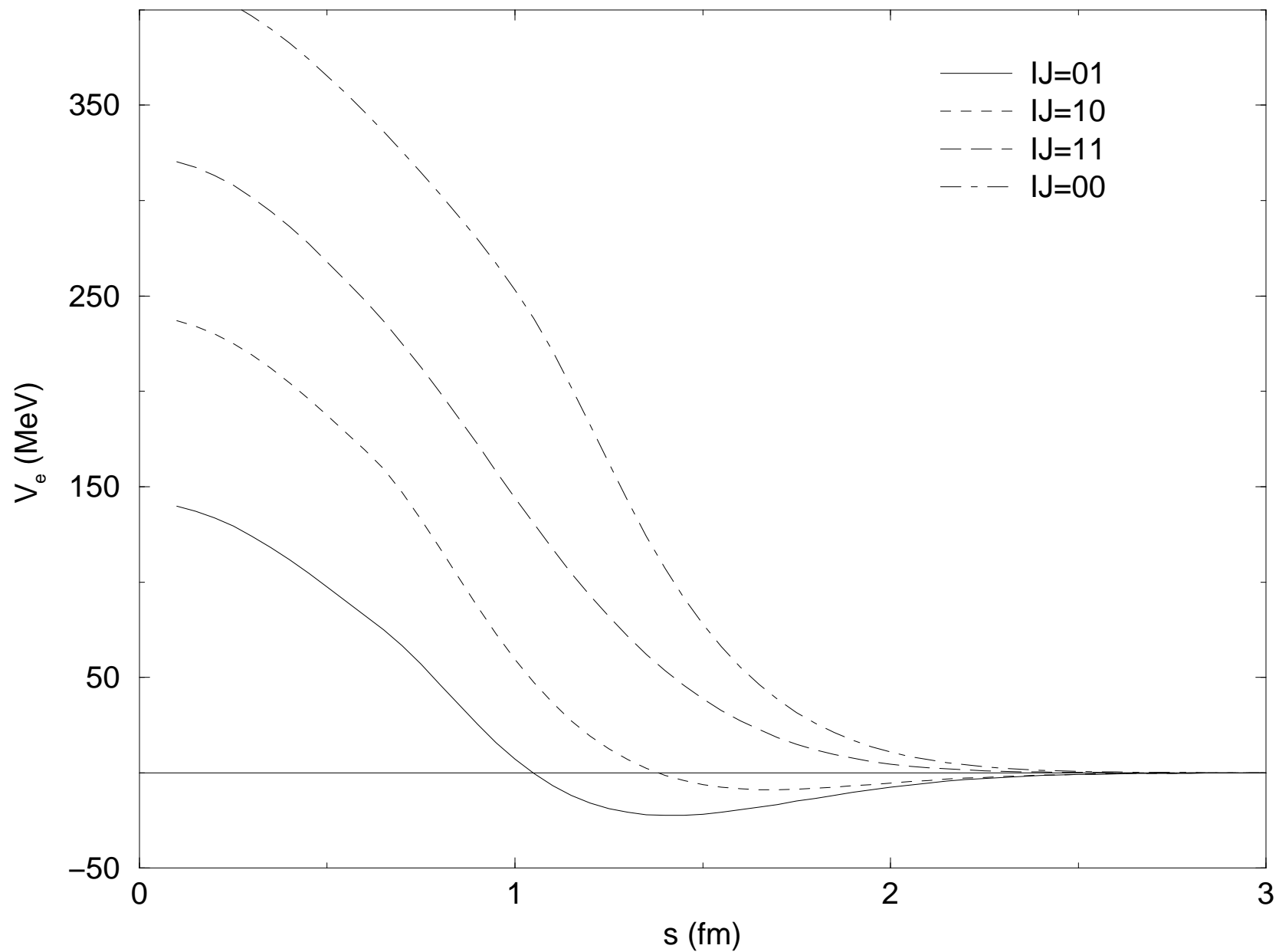


Fig.2. Effective potential
(for $N\Sigma$)

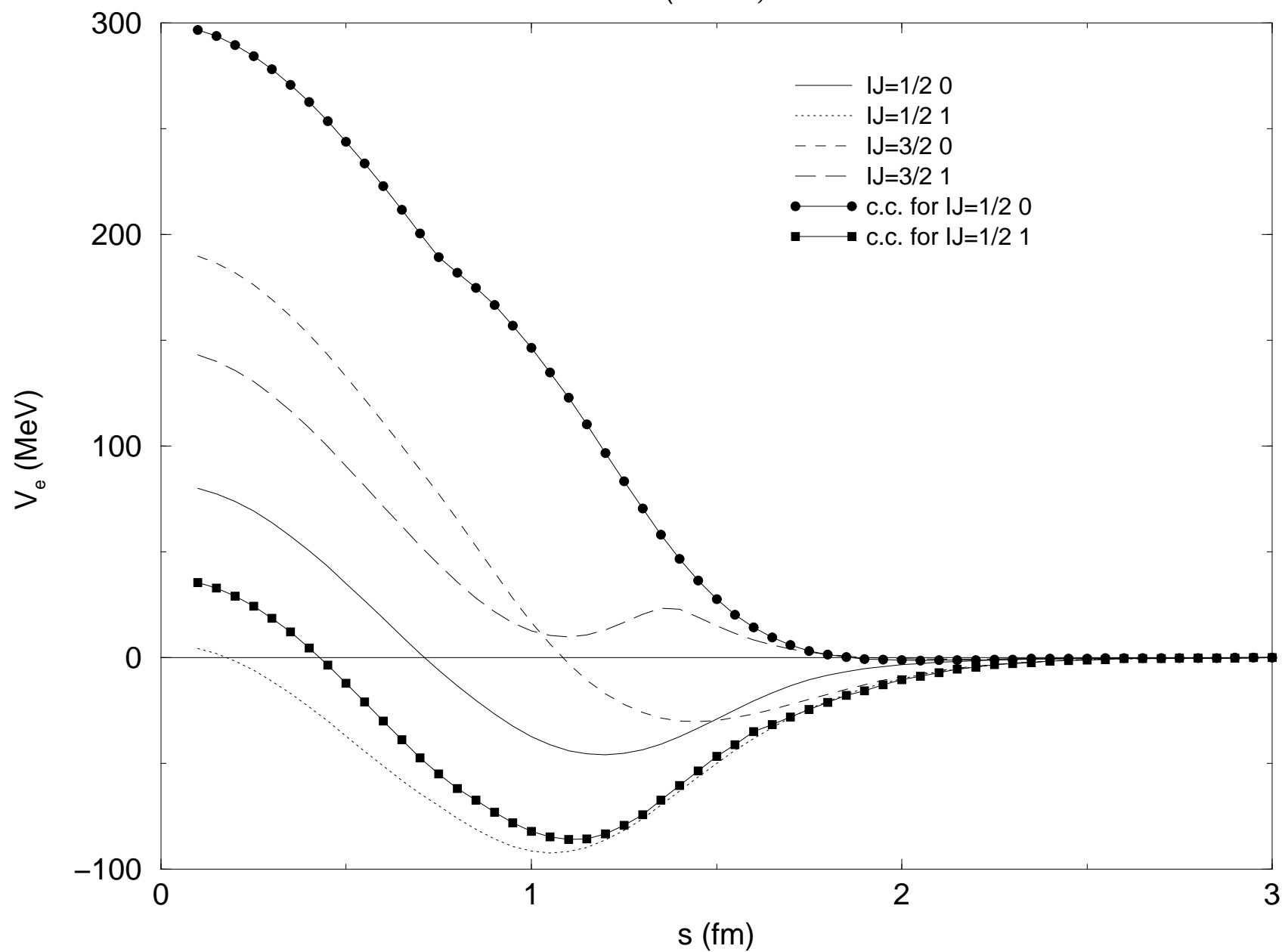


Fig.3. Effective potential

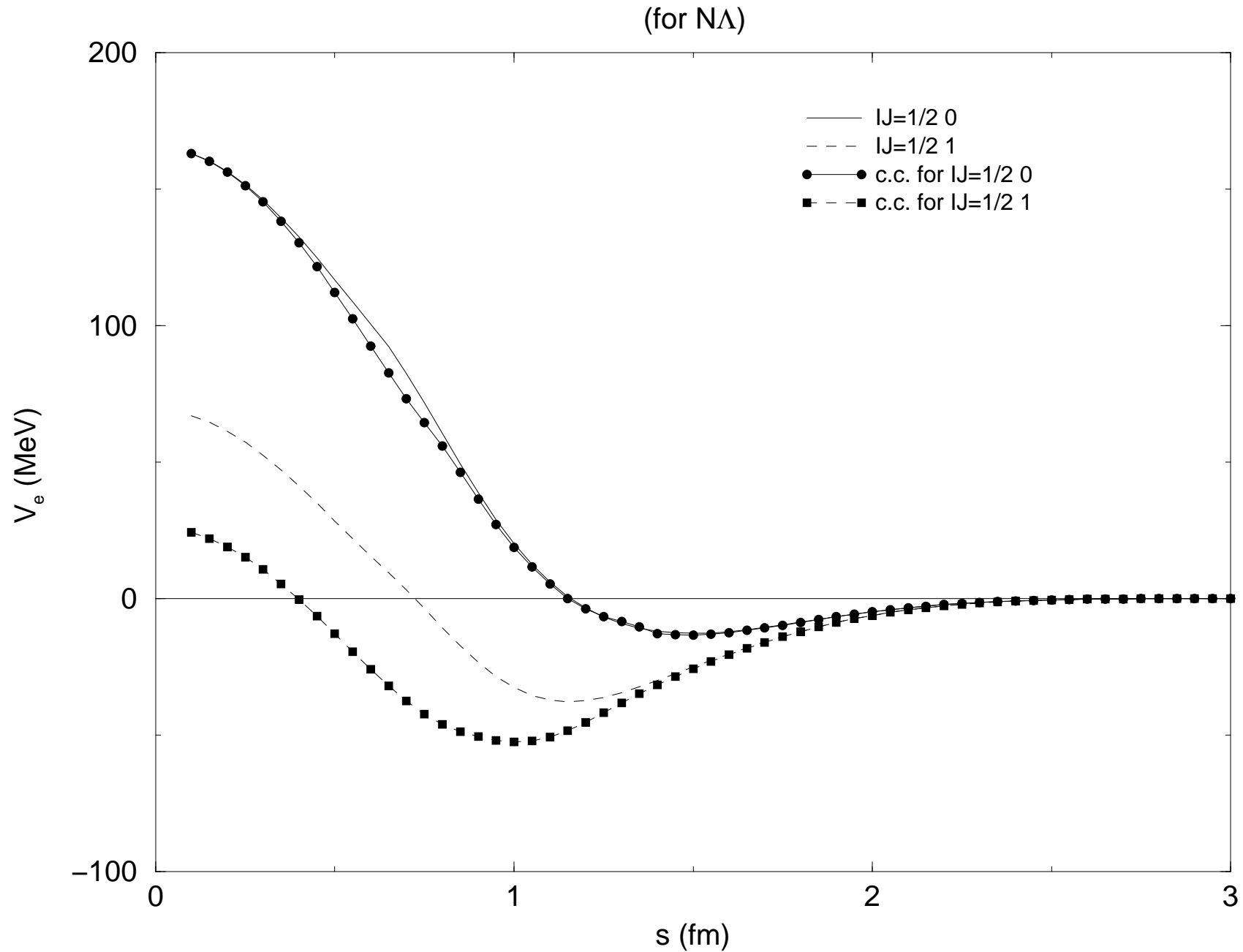


Fig.4. Effective potential

(forbidden states)

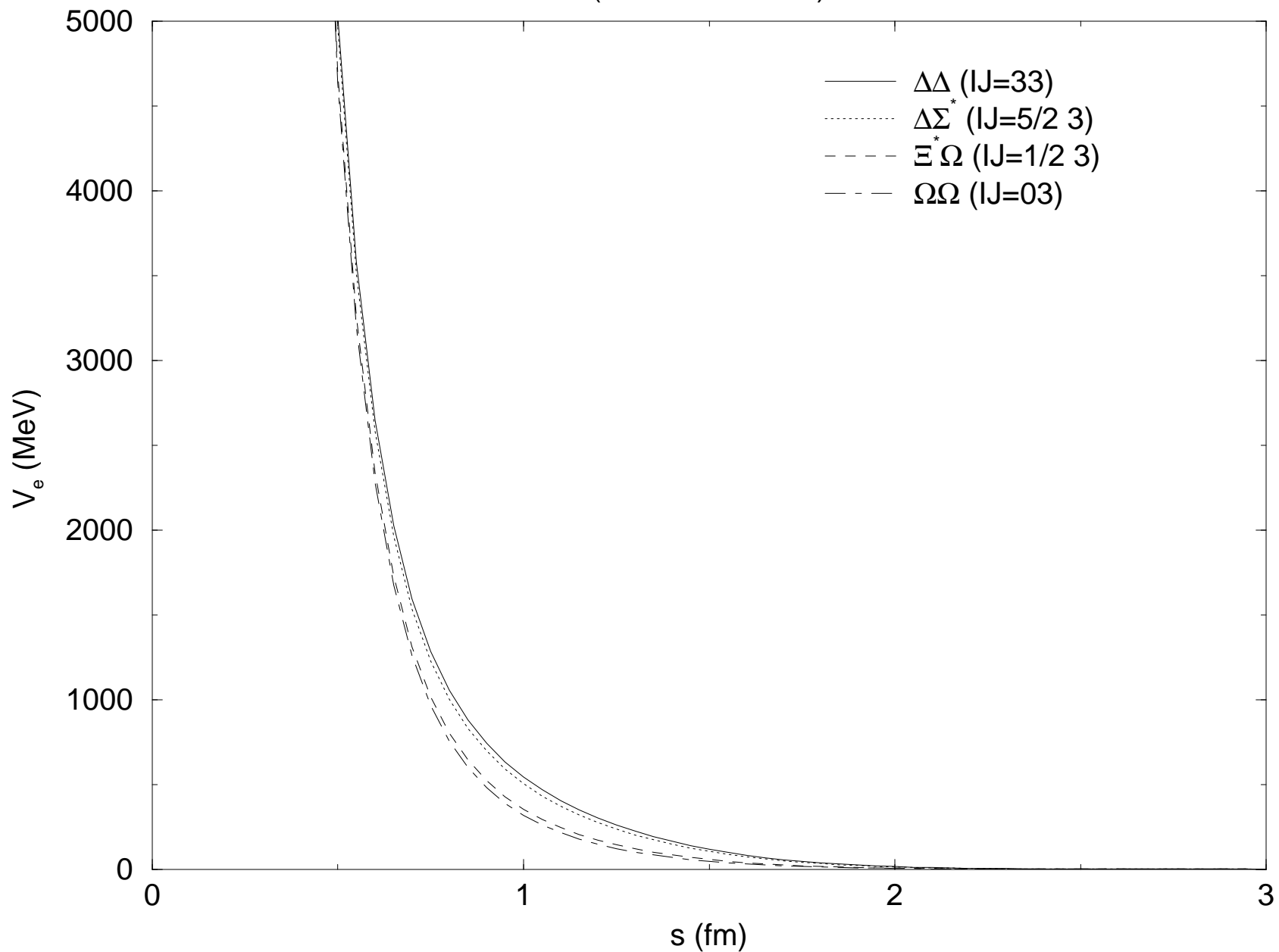


Fig. 5. Effective potential

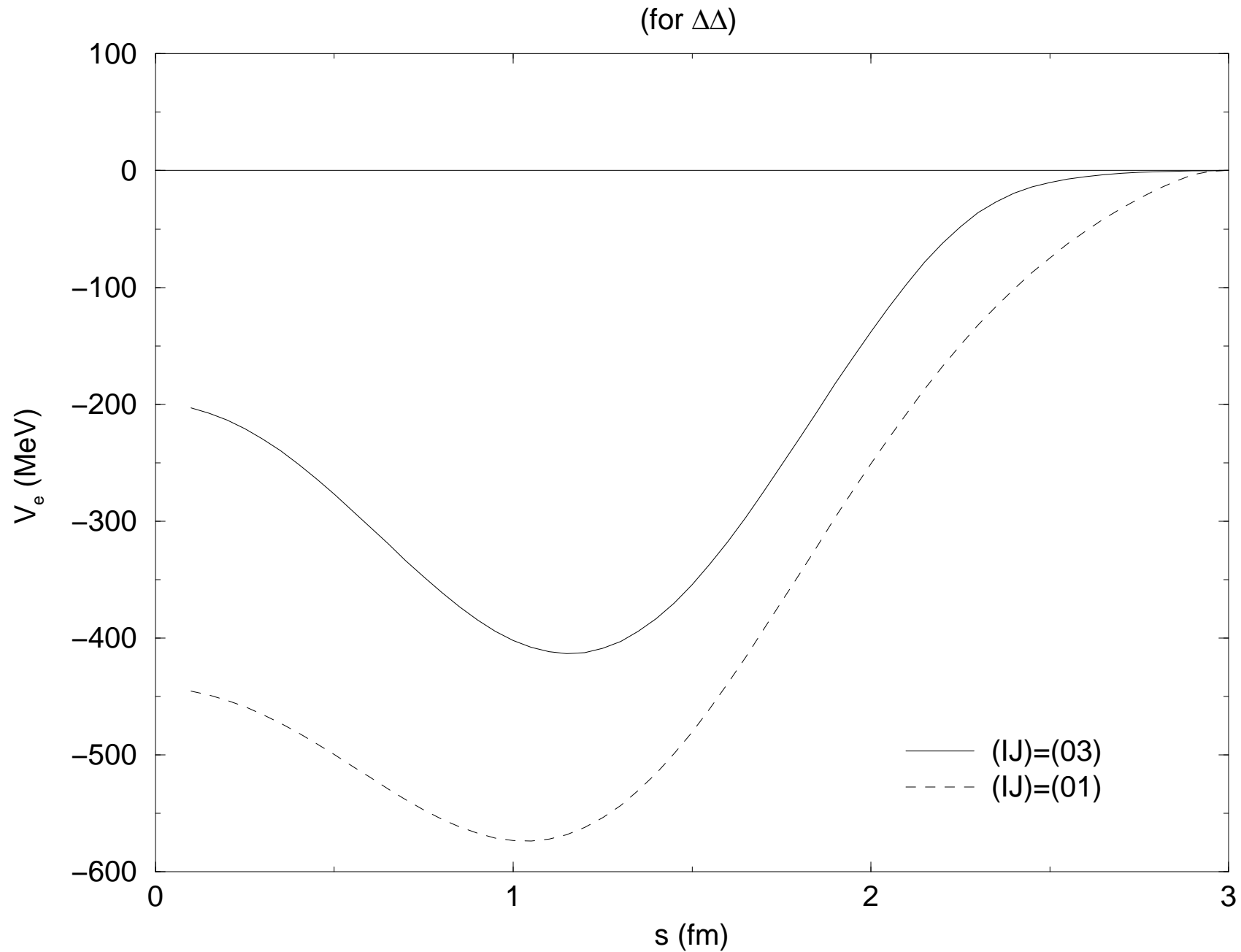


Fig.6. Effective potential
(for $YIJ=000$)

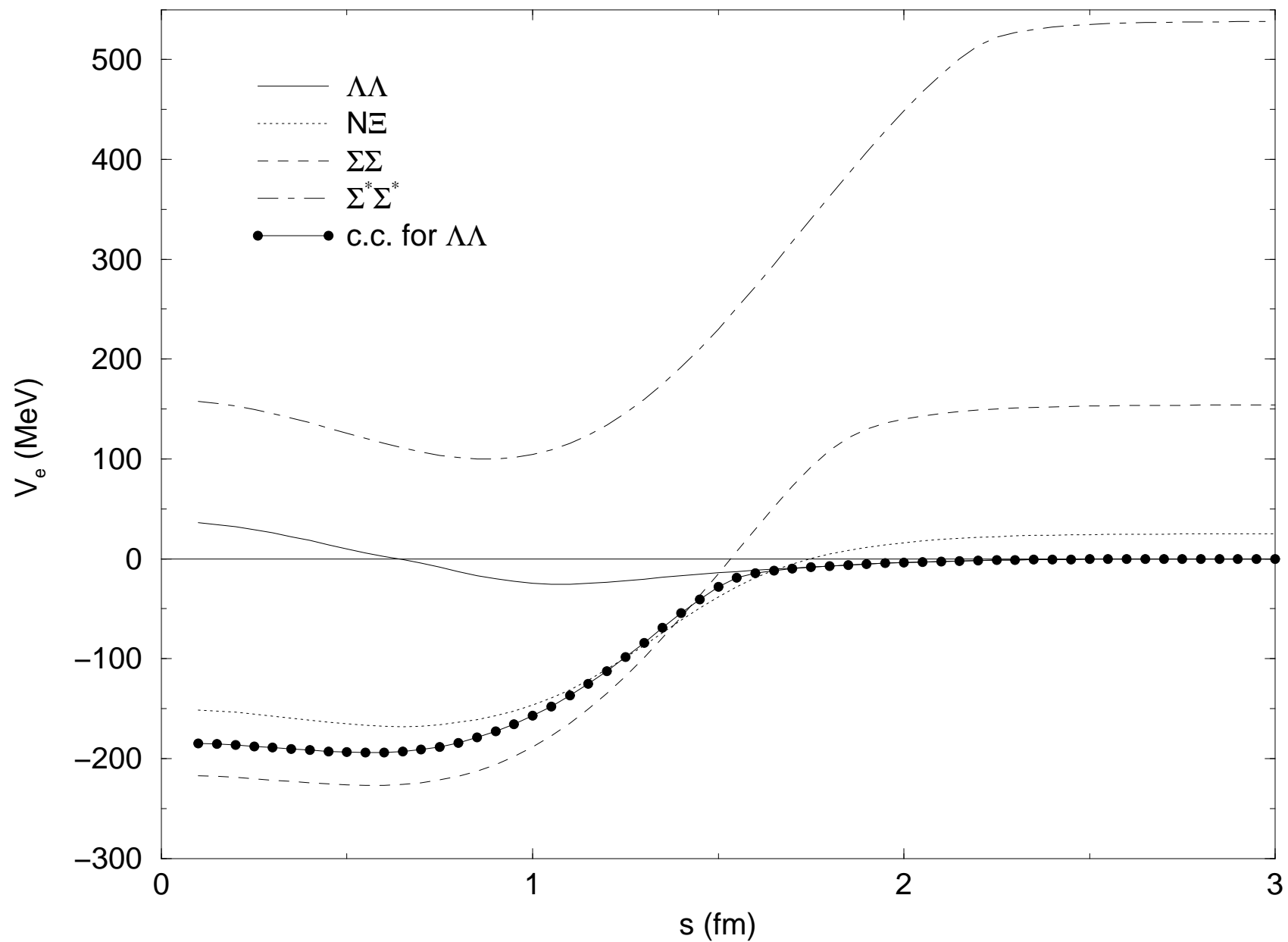


Fig.7. Effective potential
(for $N\Omega$)

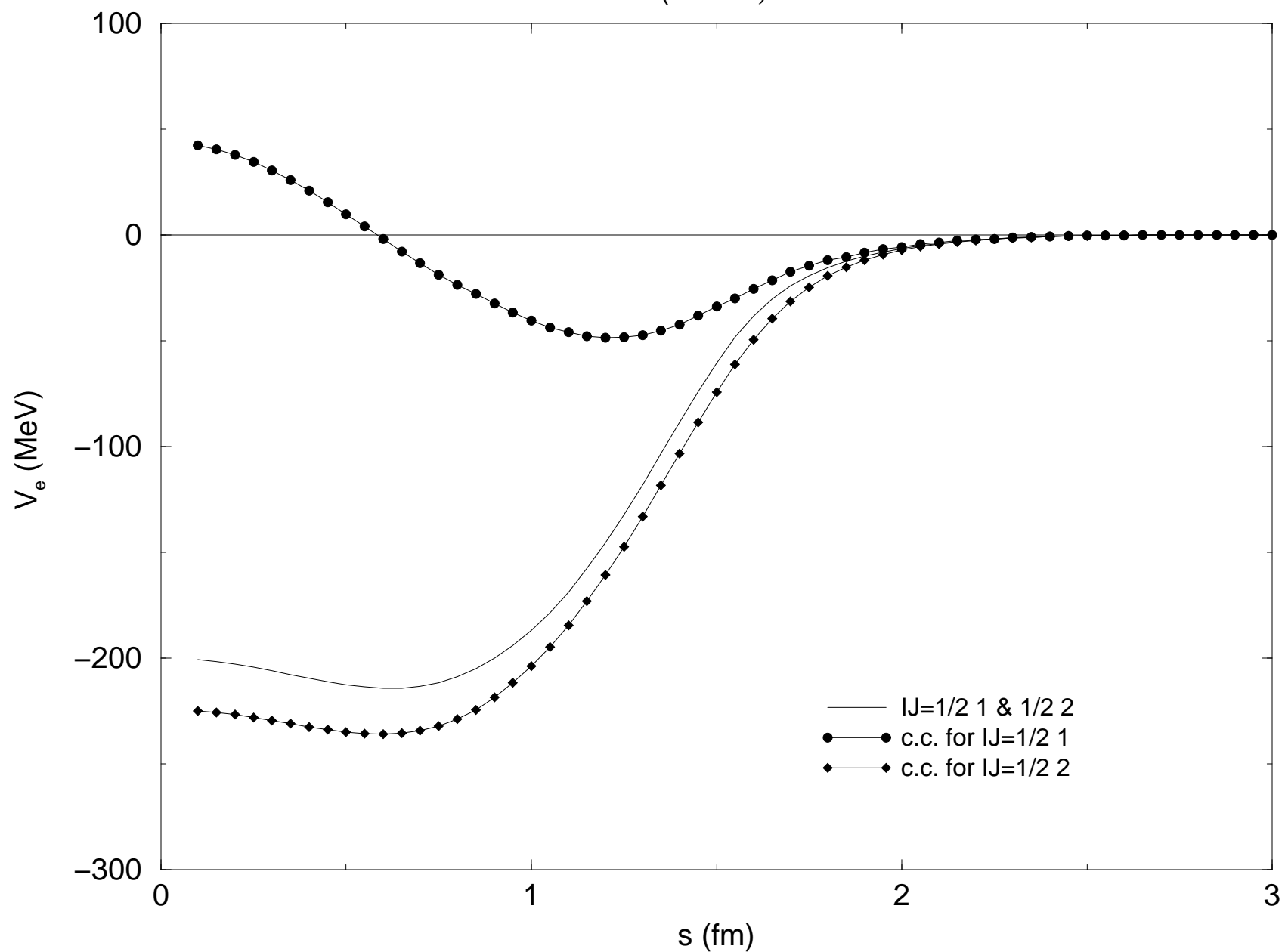


Fig.8. Effective potential

(for $\Sigma\Sigma$, $\Xi\Xi$, $\Omega\Omega$)

